PHYSICAL REVIEW B VOLUME 23, NUMBER 2 15 JANUARY 1981

Non-Ohmic electrical conductivity and giant dielectric constant in the quasi-one-dimensional semiconductor methyltriphenylarsonium ditetracyanoquinodimethanide

Patrick M. Lenahan* and T. J. Rowland

Department of Metallurgy and Mining Engineering, University of Illinois at Urbana-Champaign, Urbana, Illinois 61801 and Materials Research Laboratory, University of Illinois at Urbana-Champaign, Urbana, Illinois 61801

(Received 26 February 1980)

Results of measurements of the resistivity ρ and the dielectric constant K of the one-dimensional organic semiconductor methyltriphenylarsonium ditetracyanoquinodimethanide are described. Large single crystals of the highly purified compound were grown and ρ determined as a function of temperature T; K was measured over a range of both T and frequency. The activation energy for both ρ and K is found to be the same, 0.41 eV. The resistivity is non-Ohmic and the dielectric constant is quite large. We develop a model which explains the magnitude and temperature dependence of both the non-Ohmic conductivity and the dielectric constant in terms of charged barriers resulting from imperfections (including impurities) in the crystal. The presence of these barriers is verified semiquantitatively using nuclear and electron-spin resonance.

I. INTRODUCTION

Two of the more interesting macroscopic phenomena observed in TCNQ salts (and in one-dimensional conductors in general) are non-Ohmic electrical conductivity[1-13] and an extremely large, highly anisotropic dielectric constant.[14-21] A large number of publications have appeared recently discussing possible explanations for both phenomena.

Explanations for the non-Ohmic behavior include: solitons of pinned charge-density waves,[4,12,13] depinning of charge-density waves,[11] space-charge-limited current,[1,2] and phonon-assisted hopping through random barriers.[5] The giant dielectric constant has been explained in terms of several mechanisms: displacement of charge-density waves,[14,15] disorder,[16,17] and interruptions of the conducting strands.[18-20]

We have observed both a giant dielectric constant and non-Ohmic conductivity in methyltriphenylarsonium ditetracyanoquinodimethanide $Me\phi_3As(TCNQ)_2$, a highly one-dimensional semiconductor[22] with a Peierls crystal structure.[23] We have evaluated our observations in terms of the published models and find that none of them adequately explain our data.

We propose a model, based upon electrostatic barriers along the conducting TCNQ strands, which explains both the non-Ohmic behavior and the dielectric constant. Measurements of the electrical conductivity and the dielectric constant together with electron and nuclear magnetic resonance provide very strong corroborative evidence for the model.

II. CRYSTAL GROWTH

We have grown large (up to about $2 \times 2 \times 0.4$ cm^3), high-quality, single crystals of $Me\phi_3As(TCNQ)_2$ using the method of Melby *et al.*[24] but incorporating a number of refinements. Examples of the crystals grown are shown in Fig. 1. The TCNQ was multiply gradient sublimed, and the methyltriphenylarsonium iodide was multiply recrystallized from solution. The final single crystals were grown from highly purified acetonitrile in a dry argon atmosphere. Details of the crystal-growing procedure will be published elsewhere.[25] The structure of these crystals[2] was confirmed by x-ray analysis; the relationship between crystal-axis directions and the external surfaces of the macroscopic crystals is shown in Fig. 2.

III. NON-OHMIC CONDUCTIVITY

A. Data and comparison with previously published models

We have observed deviations from Ohm's law in the single crystals of $Me\phi_3As(TCNQ)_2$ grown as described above. A number of experimental[1-10] and theoretical[5,11-13] papers have appeared in recent years discussing such deviations in one-dimensional conductors. The explanations thus far offered for this behavior include: the excitation of solitary waves in a weakly pinned charge-density wave (CDW) system,[4,12,13] depinning of charge-density waves,[11] space-charge-limited current,[1,2] and phonon-assisted hopping through random barriers.[5] One of the goals of this research has been to determine which, if any, of the published models properly describes the non-Ohmic conductivity observed in $Me\phi_3As(TCNQ)_2$.

We have made both two- and four-probe resistivity measurements on more than a dozen of our single crystals of $Me\phi_3As(TCNQ)_2$. Electrical contact to the crystals was made with silver paint. We find that in the high-conductivity direction, the current increases more rapidly with increasing

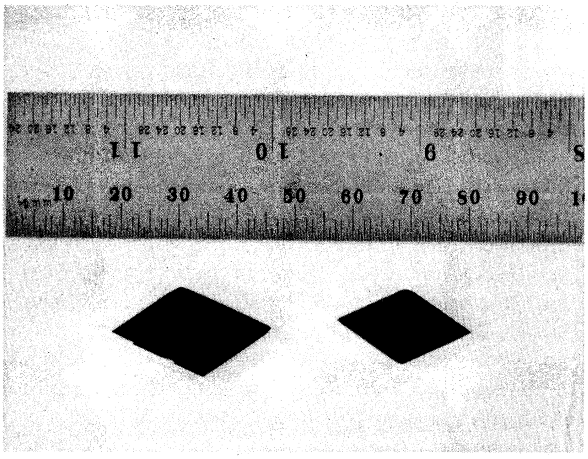

FIG. 1. Two typical crystals of $Me\phi_3As(TCNQ)_2$ as described in the text and used in this study.

voltage than predicted by Ohm's law. The deviation from Ohm's law occurs at applied fields of about 7 V/cm; this is a very small field in terms of most atomic-scale processes. The electrical behavior of several crystals is shown in Figs. 3–7 and Table I. Note that the conductivity is activated and deviates from Ohm's law only in the high-conductivity direction. It has been suggested that the non-Ohmic behavior observed in TTF-TCNQ is caused by Joule heating[26]; in order to rule out this possibility, a simple pulse technique with variable duty cycle was used at room temperature. A potential was applied for 20-μsec intervals separated by 20 msec; when the "on" time was doubled, no change in behavior was observed.

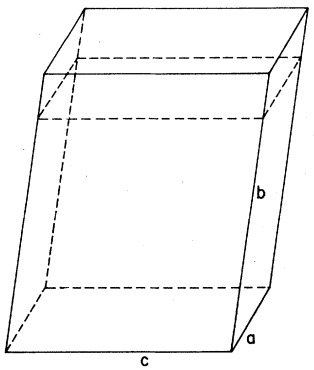

FIG. 2. Sketch of a single crystal with conventional crystal-axis designations indicated. The crystal cleaves on the plane indicated by the dashed line near the top. Thin wafers obtained from our large $Me\phi_3As(TCNQ)_2$ crystals correspond in orientation to the region above the cleavage plane indicated here. In this case the high conductivity axis b is approximately perpendicular to the plane of the cleaved wafers.

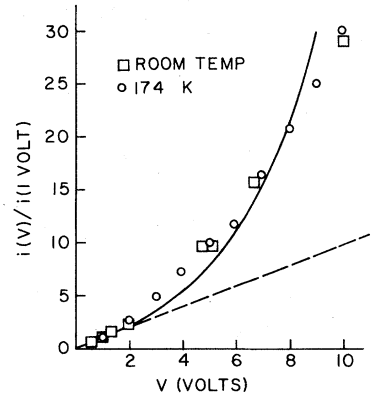

FIG. 3. Current versus voltage near the b (high-conductivity) direction. The dashed line represents Ohmic behavior with resistance determined at one volt. The solid line is taken from Eq. (9), with $V_0 = 0.2$ eV, $\lambda = 10$, $c = 270$ cm^{-1}. The plot of $i(V)/i(1$ volt) is for both room temperature and 174 K. This a "two-probe" measurement on a crystal 0.17 cm thick with cross-sectional dimensions 0.18×0.45 cm^2.

As shown in Fig. 3 and Table 1, the proportional deviation from Ohmic behavior $R(V)/R(1$ volt) is temperature *independent*. Generally, the non-Ohmic behavior observed by others is temperature *dependent*, with the deviation from Ohmic behavior becoming more pronounced as the temperature is lowered.

The model based on the depinning of charge-density waves and that based upon phonon-assisted hopping through random barriers both predict the behavior of current I to be of the form[5,11]

$$I = I_0 e^{-\Delta/kT} \sinh \frac{eE\lambda}{kT}, \tag{1}$$

where E is the electric-field strength, Δ is the activation energy of conduction, and λ is a characteristic length. In the CDW model, λ is the Peierls wavelength ($\simeq 12$ Å); in the phonon-assisted

TABLE I. The data in this table come from four-probe resistivity measurements on a crystal of $Me\phi_3As(TCNQ)_2$ which was 1.2 cm long with cross-sectional dimensions 0.1×0.2 cm^2. The high-conductivity axis was approximately parallel to the long direction. The current electrodes were separated by 1.2 cm and the voltage electrodes were separated by 0.3 cm. Resistance is measured at 7 V/cm and 24 V/cm at several temperatures; the ratio of resistances is given below.

Temperature (K)	$\frac{R(24\ \text{V/cm})}{R(7\ \text{V/cm})}$
294	0.59
245	0.62
170	0.66

hopping model λ is the distance between barriers (strand interruptions). For $Me\phi_3As(TCNQ)_2$ the dependence on temperature of current versus applied voltage (cf. Fig. 3 and Table I) is functionally different from Eq. (1). This is true for any value of the variables in Eq. (1); thus there appear to be no circumstances under which our data are described by Eq. (1), and we conclude that the depinning of CDW's and phonon-assisted hopping do not play an important role in our investigation.

The basic properties of space-charge-limited currents i(SCLC) can be approximately determined quite readily for the case of a flat planar geometry.[27,28] The space charge Q(SCLC) injected into a crystal of thickness d, is given roughly by the product of its geometrical capacitance ($C = \epsilon_0 KAd^{-1}$, where ϵ_0 is the permittivity of free space, K the dielectric constant, and A the cross-sectional area) and the applied voltage V; thus Q(SCLC) $\simeq V\epsilon_0 KAd^{-1}$. The time required for the injected space charge to cross the crystal is the charge-carrier transit time $\tau = d^2/\mu_T V$, where μ_T is the time-of-flight mobility. The space-charge-limited current is the injected charge divided by the transit time of i(SCLC) $\simeq \epsilon_0 KAV^2\mu_T d^{-3}$.

We may crudely estimate the mobility required for the onset of the SCLC non-Ohmic behavior to occur at a given threshold field E_T by equating the space-charge density with the charge-carrier density at zero field. If the conductivity at very low field is given by $\sigma = ne\mu_T$, where n is charge-carrier density and e is electronic charge, $\sigma/\mu_T = ne$ and $\mu_I \simeq \sigma d/(\epsilon_0 KE_T)$. From the data of Fig. 4 at room temperature $\sigma \simeq 3\times10^{-4}$ $(\Omega\,\mathrm{cm})^{-1}$, $d \simeq 0.17$ cm, and as discussed below, $K \simeq 5\times10^3$. Since from Fig. 3, $E_T \simeq 7$ V/cm, a mobility of order

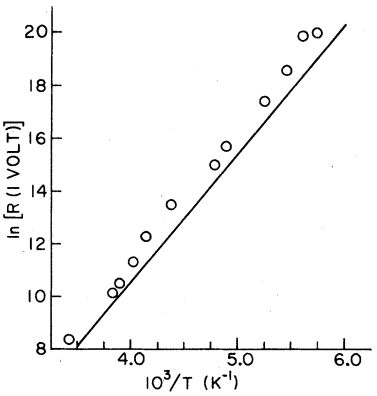

FIG. 4. Plot of ln (R) ($R = 1$ volt/i) versus reciprocal temperature for the case of one volt applied. The solid line is obtained using Eq. (9) with $V_0 c$ as given in the caption of Fig. 3 and $\Delta = 0.41$ eV. The data are from the crystal of Fig. 3.

10^4 cm^2/V sec would be required for SCLC to be the cause of the non-Ohmic behavior. To the best of our knowledge,[29] no mobility larger than about 10 cm^2/V sec has been reported in the literature for organic materials. Thus SCLC is not likely to be the cause of the non-Ohmic conductivity.

The SCLC model predicts a characteristic transient response[30] to a pulse of applied voltage. The transient (for the planar geometry discussed earlier) includes a cusp, or a maximum, at approximately a transit time after the application of the pulse. Using a sampling scope and a pulse generator with about a 1-nsec rise time we were unable to observe the predicted transient. On the basis of the dc and transient experiments we conclude that space-charge-limited currents do not contribute significantly to the observed non-Ohmic behavior.

The discussion of Cohen and Heeger[8] suggests to us that if the non-Ohmic conductivity is caused by solitons, the deviations from Ohm's law should appear gradually as the temperature is lowered. In systems where the soliton model is appropriate the activation energy of conduction is a function of applied field. As can be deduced from Fig. 3 and Table 1, this is not the case for $Me\phi_3As(TCNQ)_2$. Thus the soliton model used by Cohen and Heeger appears to be not applicable to $Me\phi_3As(TCNQ)_2$.

The activation energy for conduction derived from Fig. 4 is 0.41 eV. Figures 5, 6, and 7 display, respectively, i vs V near the stacking direction b and near the two directions a and c perpendicular to it.

B. Theory: Tunneling model

We propose a tunneling model, based upon electrostatic (Coulomb) barriers caused by charged imperfections distributed along the conducting TCNQ strands. The Wentzel-Kramers-Brillouin (WKB)[31] approximation is then used to calculate the current in a single, imperfect strand.

The height of the Coulomb barriers is obtained by taking the Coulomb repulsion energy (e^2/r) equal to that of two electrons separated a distance r of 10 Å (the same as that between the ends of a TCNQ molecule). A value of about 1 eV is obtained. When one takes into account the effect of the associated cations $(Me\phi_3As)^+$ a somewhat smaller value would be expected. LeBlanc[32] estimates that the presence of these heterocyclic cations reduces the repulsive energy of two electrons on one TCNQ molecule by a factor of about 5. Our situation is fundamentally similar; we assume the height of the barrier to be approximately 0.2 eV. A rough estimate of the width of the barrier can be had by realizing that the poten-

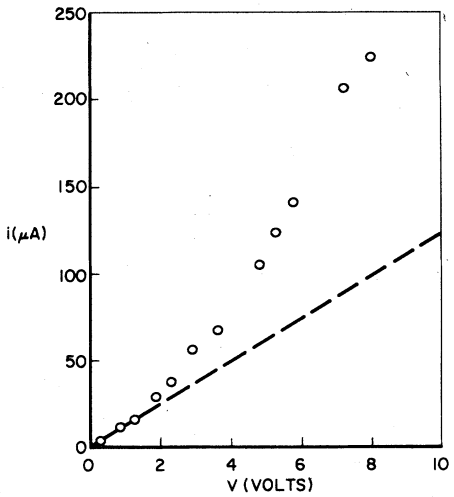

FIG. 5. Current versus voltage from a "four-probe" resistivity measurement at room temperature. The crystal is 0.8 cm in length with cross-sectional dimensions 0.1×0.1 cm^2. The current leads are separated by the length of the crystal (0.8 cm). The voltage leads are separated by 0.2 cm. The high-conductivity direction in the crystal corresponds to the direction in which it is 0.8 cm long. The dashed line represents Ohmic behavior with resistance determined at 0.91 V. The four probe measurement shows that the non-Ohmic behavior is not a result of non-Ohmic electrical contacts.

tial will be of the general form e^2/r. Assuming that the distance of closest approach between the conduction electron and the electron on the imperfection is 10 Å, a reasonable width is of order 20 Å. The model barrier is illustrated in Fig. 8. In addition, the bandwidth is assumed to be considerably smaller than the barrier height; Conwell[33] apparently considers 0.04 eV a reasonable

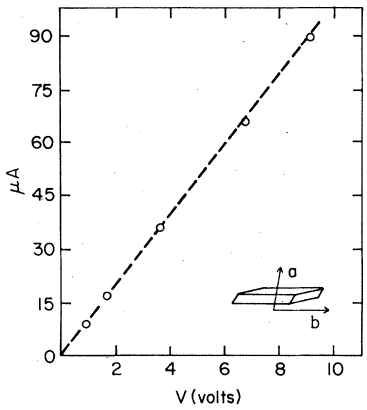

FIG. 6. Current versus voltage near the *a* direction. This is a two-probe measurement taken at room temperature on a crystal 0.08 cm thick with approximate cross-sectional area 0.57×0.45 cm^2. Note that in this direction, Ohm's law is obeyed up to at least 100 V/cm.

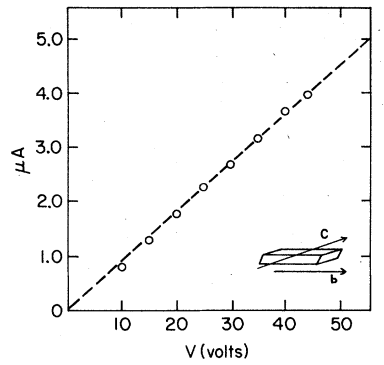

FIG. 7. Current versus voltage near the *c* direction. This is a two-probe resistivity measurement taken at room temperature on a crystal 0.31 cm thick with approximate cross-sectional dimensions 0.20×0.16 cm^2. Note that in this direction Ohm's law is obeyed up to at least 140 V/cm.

estimate in similar compounds. The effect of screening on the barriers will be taken into account using the Thomas-Fermi model.

Using the WKB method to determine the charge tunneling through the barrier, we assume that the total voltage applied across the crystal is the sum of equal drops across each barrier in any chain (see Fig. 8). The current flowing in a TCNQ stack will be proportional to the difference between the transmission coefficients in the "forward" and "reverse" directions. In the forward direction, the WKB method gives a transmission coefficient

$$\theta_1 = \frac{|\psi(x=a_0)|^2}{|\psi(x=0)|^2}$$

$$= \exp\left(-\frac{2}{h}\int_0^{a_0} [8\pi^2 m \Delta V(x)]^{1/2} dx\right). \qquad (2)$$

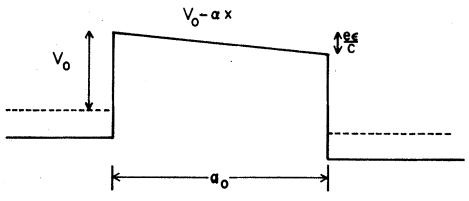

FIG. 8. Electrostatic barriers along the conducting chains are represented as rectangular and of height V_0 above the electronic energy (band) level. When a potential is applied across the conducting strand, the potential drop is assumed to take place across the barrier as shown. (The dashed lines schematically indicate the narrow conduction band.)

We evaluate the integral using $\Delta V(x) = V_0 - \alpha x$, where $\alpha = e\epsilon/ca_0$, a_0 is the barrier width, c is the number of barrier imperfections per unit length along the chain, and e is the absolute value of the electronic charge. The parameter ϵ is the voltage applied across the crystal divided by the length of the crystal in the chain direction, and m is the electronic mass.

We consider the case $\alpha x < V_0$, thus, expanding in $\alpha x/V_0$, the integrand may be expressed

$$(8\pi^2 m V_0)^{1/2}\left[1-\left(\frac{\alpha}{2V_0}\right)x-\frac{1}{2}\left(\frac{\alpha}{2V_0}\right)^2 x^2-\cdots\right], \tag{3}$$

and the value of the exponent is approximately

$$\gamma\left(\frac{e\epsilon}{4V_0 c}+\frac{e^2\epsilon^2}{24V_0^2c^2}-1\right),$$

where

$$\gamma=\frac{2}{h}(8\pi^2 m)^{1/2}V_0^{1/2}a_0. \tag{4}$$

We have a forward transmission coefficient of the form

$$\theta_1=\exp\left[\gamma\left(\frac{e\epsilon}{4V_0c}+\frac{e^2\epsilon^2}{24V_0^2c^2}-1\right)\right]. \tag{5}$$

The electronic energy levels on the low side of the barrier will be approximately $\alpha a_0 = e\epsilon/c$ lower than on the high side. The first-order approximation used in deriving Eq. (5) also was used to obtain the reverse transmission coefficient. In this case $\Delta V(x) = V_0 + e\epsilon/c - \alpha x$. Thus

$$\theta_2=\exp\left[\gamma\left(\frac{-e\epsilon}{4V_0c}+\frac{e^2\epsilon^2}{24V_0^2c^2}-1\right)\right], \tag{6}$$

and

$$\Delta\theta=(\theta_1-\theta_2)$$

$$=\left[1-\exp\left(\frac{-\gamma e\epsilon}{2V_0c}\right)\right]\exp\left[\gamma\left(\frac{e\epsilon}{4V_0c}+\frac{e^2\epsilon^2}{24V_0^2c^2}-1\right)\right]. \tag{7}$$

The current will be equal to the product of $\Delta\theta$ and the number of charge carriers incident on the barrier per unit time. A zero-order estimate of the magnitude of the current can be obtained by considering the electron velocity to be of order $v=(3kT/m)^{1/2}$ and the concentration of charge carriers per unit length $n=(2d)^{-1}\exp(-\Delta/kT)$, where Δ is the activation energy of conductivity. The cations donate one electron per every two TCNQ molecules; the latter are spaced about $d=3.3$ Å apart. In a length l of a conducting strand there will be about nl electrons, each of which will impinge on the barrier at roughly the frequency v/l. We obtain an admittedly crude estimate for the number of charge carriers incident on the barrier per unit time nv, and thus have an approximate expression for the current in a conducting strand:

$$i=nev\,\Delta\theta=C_0T^{1/2}\exp\left(\frac{-\Delta}{kT}\right)\left[1-\exp\left(\frac{-\gamma e\epsilon}{2V_0c}\right)\right]$$
$$\times\exp\left[\gamma\left(\frac{e\epsilon}{4V_0c}+\frac{e^2\epsilon^2}{24V_0^2c^2}\right)\right], \tag{8}$$

where

$$C_0=\left(\frac{e}{2d}\right)\left(\frac{3k}{m}\right)^{1/2}.$$

The current in a single strand is given by Eq. (8). To find the current in a crystal of cross-sectional area A cm^2, we multiply i by the product of the number of strands per square centimeter ($\simeq 10^{14}$) and the area A. Thus,

$$I(\epsilon)=A10^{14}i. \tag{9}$$

It is worth pointing out that the model predicts non-Ohmic behavior to occur in *semi*conductors, not metals. The Coulomb potential will be screened to some extent by a redistribution of conduction electrons. One may take the Thomas-Fermi screening length[34] $\lambda \simeq 4\times10^{-5}L^{-1/6}$ cm$^{1/2}$, where L is the number of charge carriers per unit volume, as an extremely rough estimate of the range of the screening. We assume an unscreened barrier on the order of 20 Å in width. If the number of charge carriers per unit volume were that of copper ($L = 8.5\times10^{22}$ cm^{-3}), $\lambda \simeq 0.55$ Å; if $L = 10^{21}$ cm^{-3}, $\lambda \simeq 1.3$ Å. Clearly, a 20-Å Coulomb barrier would be virtually obliterated by screening if $L \simeq 10^{21}$ cm^{-3}. However, if $L = 10^{14}$ cm^{-3}, $\lambda \simeq 19$ Å and the barrier would be essentially unscreened.

This crude argument predicts that the non-Ohmic behavior would not be observed in one-dimensional metals. Experimentally, the non-Ohmic behavior is *not* obserbed in one-dimensional metals. In one-dimensional metals which undergo a metal-to-semiconductor transition [tetrathiofulvalene tetracyanoquinodimethane and quinolinium (tetracyanoquinodimethane)$_2$], the non-Ohmic behavior appears only below the transition to semiconducting behavior.[5,8,10] In one-dimensional semiconductors with very small activation energies of conduction (in which the charge-carrier density at high temperatures might approach that of a metal) the non-

Ohmic behavior appears only gradually as the temperature is lowered.[4] The model presented thus qualitatively predicts the behavior previously observed in other one-dimensional systems.

The $Me\phi_3As(TCNQ)_2$ crystals have relatively modest conductivity. Even at room temperature, where $\sigma \simeq 3 \times 10^{-4}$ $(\Omega\ \mathrm{cm})^{-1}$, we would not expect screening to affect significantly the shape of the barriers proposed in our model.

C. Experimental measurement of imperfection concentration

We measure the unpaired electron concentration, which we associate with imperfections, by means of low temperature (2.0 to 4.2 K) proton spin-lattice relaxation time T_1 measurements, and also by electron-spin-resonance absorption amplitude measurements.

Using the scheme of saturating and subsequently sampling the proton spin magnetization, we find $T_1 \simeq 100$ sec in single crystals at 4.2 K; T_1 changes little as the temperature is lowered to 2.0 K. Essentially the same T_1 is found in crystals in which the hydrogen sites on the TCNQ molecules are deuterated. The effect on T_1 of paramagnetic impurities in diamagnetic insulating crystals is to decrease T_1 through nuclear spin diffusion. The impurities act as energy sinks to the crystal lattice. Bloembergen[35] has calculated the spin-diffusion coefficient $D \simeq a^2/(50T_2)$, where a is the separation distance of the active nuclei and T_2 is the nuclear spin-spin relaxation time. The relationship between paramagnetic impurity concentration per unit volume N and T_1 is approximated[36] by $T_1^{-1} \simeq 4\pi NaD$; therefore $N \simeq 50T_2/(4\pi a^3 T_1)$.

From cw NMR line width measurements, we find $T_2 = 2.1 \times 10^{-5}$ sec. If we take $a \simeq 2.5$ Å, we obtain $N \simeq 5.3 \times 10^{16}$ cm^{-3} and we estimate the fraction f of TCNQ sites with negatively charged imperfections to be $f \simeq 1.4 \times 10^{-5}$.

We have also obtained a rough measure of the imperfection concentration through ESR measurements on several single crystals of $Me\phi_3As(TCNQ)_2$ at 95 K. The major portion of the ESR signal in $Me\phi_3As(TCNQ)_2$ has been attributed to triplet excitons.[37] As the temperature is lowered, the exciton resonance first broadens, then splits. Generally some small intensity remains at the center. This center resonance is attributed to "impurities" in TCNQ compounds.[38] The triplet resonance intensity is an exponential function of temperature with an activation energy J; the exchange integral $J \simeq 0.062$ eV. We estimate the fraction of electrons in the excited state to be $3\exp(-J/kT)$,[37] and compare the integrated intensity I of the imperfection resonance to that of the exciton resonance. Assuming (from the NMR measurements on selectively deuterated crystals) that half of the imperfections are on the conducting TCNQ chains, and that there is one unpaired electron for every two TCNQ molecules at high temperature, we estimate the fraction f of TCNQ sites with unpaired electron impurities to be given by

$$f \simeq \frac{3}{4} \frac{I(\text{imperfection})}{I(\text{exciton})} \exp\left(\frac{-J}{kT}\right). \tag{10}$$

A typical ESR spectrum is shown in Fig. 9; this crystal was grown in the same batch as the one used for the conductivity measurements plotted in Figs. 3 and 4. From that spectrum (obtained at 95 K) we find $f \simeq 1.2 \times 10^{-5}$.

Both the ESR and NMR yield approximately the same results: a concentration of unpaired electron imperfections of about 10^{-5}. The measurements should be regarded as accurate to no better than a factor of 2.

D. Quantitative evaluation of model

Having experimentally determined the approximate number of charged imperfections, and estimated the values for V_0 and a_0, the value of every quantity in Eq. (9) is approximately known: $c = f/(3.3 \times 10^{-8}) \simeq 300$ cm^{-1}, $V_0 \simeq 0.2$ eV, $a_0 \simeq 20$ Å, and $\gamma \simeq 10$. If we let $\gamma = 10$, $f = 9 \times 10^{-6}$ ($c = 270$ cm^{-1}), and $V_0 = 0.2$ eV in Eq. (9), a good fit to the data of Figs. 3 and 4 is obtained.

In view of the approximate nature of the calculation, the fit between theory and experiment is good; furthermore, our data do not appear to be adequately explained by any of the models referred to earlier.[11-13] In addition, the model may qual-

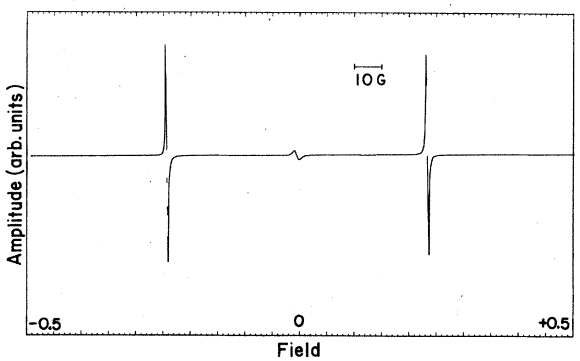

FIG. 9. Electron spin resonance absorption derivative spectrum taken at $T = 95$ K and $\nu = 9.1$ GHz. The small signal in the center is generally associated with imperfections. The two larger resonances are due to triplet excitons on the TCNQ as discussed in Refs. 37 and 38.

itatively describe much of the non-Ohmic behavior observed by others, including its disappearance as temperature is increased.

IV. DIELECTRIC CONSTANT

A. Experimental results

The dielectric constant of $Me\phi_3As(TCNQ)_2$ was measured in the high-conductivity direction as a function of frequency and temperature. It is possible to obtain thin wafers of $Me\phi_3As(TCNQ)_2$ by cleaving larger crystals. The plane surfaces of the cleaved wafers are approximately perpendicular to the high-conductivity direction as indicated in Fig. 2.

The dielectric constant of these wafers was measured over a range of frequency and temperature using an rf bridge and cooled He gas in a shielded chamber. For the case of a thin slab of dielectric between two flat-plate conductors, and neglecting geometric effects, the capacitance C is given by $C = (\epsilon_0 K/d)A$; the quantities appearing are defined below Eq. (1).

The capacitance is determined from the rf bridge measurement: The crystal is treated as a resistor and capacitor in parallel. From the real ρ' and imaginary α' parts of the impedance, both the resistance R and the capacitance C are readily determined:

$$R = \rho'\left[\left(\frac{\alpha'}{\rho'}\right)^2 + 1\right], \quad C = \frac{1}{\rho'}\left(\frac{\alpha'}{\rho'\omega}\right)\left[\left(\frac{\alpha'}{\rho'}\right)^2 + 1\right]^{-1},$$

where ω is 2π times the source frequency of the rf bridge.

The dielectric constant determined from these measurements is thermally activated and frequency dependent as illustrated in Figs. 10 and 11. The activation energy for the dielectric constant is found to be the same as that for the electrical conductivity.

B. Comparison of results with predictions of previously published models

As mentioned earlier, a large dielectric constant in the high-conductivity direction is frequently observed in quasi-one-dimensional conductors. It has been attributed to several mechanisms: the displacement of the charge-density waves,[14,15] disorder,[16,17] and interruptions of the conducting strands.[18-20]

Disorder does not seem to be an important factor in $Me\phi_3As(TCNQ)_2$ crystals. In quasi-one-dimensional systems where disorder (i.e., molecular misorientation) plays an important part, the conductivity as a function of temperature is predicted to be of the form $\sigma \propto \exp[-(T_0/T)^{1/2}]$.[39] The

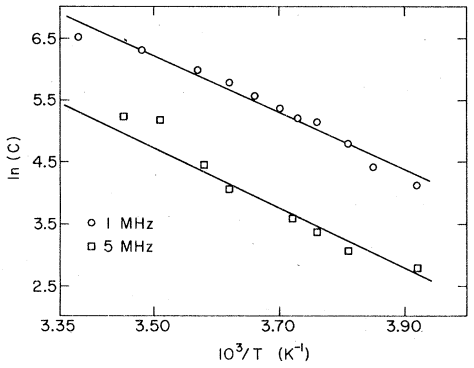

FIG. 10. Plot of ln$C$ versus reciprocal temperature. The solid lines were obtained by the method of least squares. The activation energy, determined from the slope of the lines is 0.41 eV. The crystal used had a thickness of 0.14 cm, and cross-sectional dimensions 0.57×0.43 cm^2. The dielectric constant versus frequency of this crystal at room temperature is illustrated in Fig. 11 by means of triangles.

conductivity versus temperature for $Me\phi_3As(TCNQ)_2$ has been reported in the literature several times and such a temperature dependence has not been observed.[22,40] Furthermore, the expression of Bush for the giant dielectric constant in disordered systems is essentially temperature independent.[16,17]

A dielectric constant resulting from a pinned charge-density wave would be expected to change relatively little with temperature far below the Peierls transition temperature. In fact, the phenomenological expression of Rice[14] for a giant dielectric constant caused by the displacement

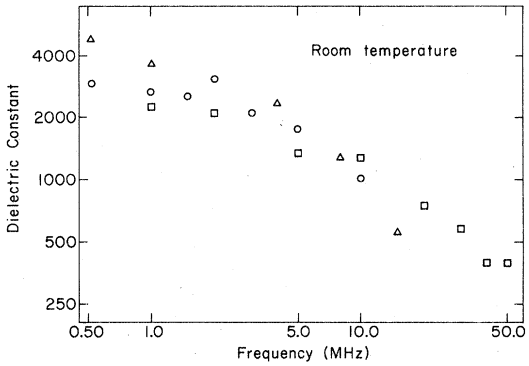

FIG. 11. Dielectric constant versus frequency for three crystals at room temperature. The triangles illustrate data of a crystal of thickness 0.14 cm and cross-sectional dimensions 0.57×0.43 cm^2; the behavior of the capacitance versus temperature of this crystal is illustrated in Fig. 10. The circles illustrate data of a crystal of thickness 0.13 cm and cross-sectional dimensions 0.61×0.23 cm^2. The squares illustrate data on a crystal of thickness 0.11 cm and cross-sectional dimensions 0.69×0.21 cm^2.

of the charge-density wave has no explicit temperature dependence if the concentration of "superfluid" electrons is taken as constant. Our measurements of the temperature dependence of the giant dielectric constant are not consistent with the predictions of the CDW model of Rice or the disorder model of Bush.

C. Barrier model

Rice and Bernasconi[18-20] developed a phenomenological model based upon barriers interrupting conducting strands for the case of a quasi-one-dimensional *metal*. We have adapted this model to the case of a semiconductor and found that it predicts a dielectric constant with the same activation energy as the conductivity. A simple derivation of the static dielectric constant is presented below.

A distribution of barriers along the conducting strands (as discussed earlier) essentially gives a crystal consisting of linear sequences of one-dimensional conducting "boxes" or wells. Solely for the sake of mathematical simplification we now consider the barriers to be insulating.

On application of a constant field E parallel to the conducting strands, the charge carriers in each box initially begin to move so that a net current is produced. After some characteristic time τ_R, corresponding to the time taken by a carrier to traverse an average box length l, charge build-up at the barriers will reduce the current flow to zero.

Phenomenologically, we may write the current-density transient just described as[19,20]

$$j(t)=\sigma_0 E[1-\exp(-t/\tau_0)]\exp(-t/\tau_R)\,, \tag{11}$$

where $\sigma_0=n_A(z/b)e^2\tau_0/m^*$ denotes the intrinsic dc conductivity of the conducting strands (in the absence of defects), τ_0 intrinsic carrier scattering time, z the number of charge carriers per one-dimensional lattice site, b the distance between lattice sites in the high-conductivity direction, and n_A the number of conducting strands per unit area perpendicular to the high-conductivity axis. The carrier effective mass is m^* and the current density is denoted by $j(t)$.

Rice and Bernasconi, considering a one-dimensional *metal* with about 1% imperfections, make several assumptions to estimate the two adjustable parameters τ_0 and τ_R. They assume that a reasonable time τ_R for the conducting segments to come into equilibrium after the application of an applied field would be $\tau_R\simeq l/v_F$: the time required for a conduction electron traveling at the Fermi velocity v_F to traverse the length l of the conducting segment. They also assume that $\tau_0 \gg \tau_R$, that the intrinsic scattering time of electrons is much longer than τ_R. These approximations lead to a static dielectric constant $K(\infty)=1+4\pi\sigma_0\tau_R^2/\tau_0$.

The foregoing assumptions are not appropriate for the crystals dealt with here. Our crystals are semiconductors, not metals. The level of impurities considered to form barriers (as discussed earlier) appears to be of order one part in 10^5 as opposed to one part in 10^2. Also a more reasonable estimate for the relaxation time τ_R may be obtained from the relation $(D_0\tau_R)^{1/2}\simeq l$, where $D_0=kT\mu_0/e$, with μ_0 being the intrinsic mobility of the charge carriers within the conducting strands. We find that $\tau_R\simeq el^2/kT\mu_0$. This τ_R is almost certainly much longer than τ_0; we assume $\tau_0\ll\tau_R$. Thus, we arrive at the phenomenological expression

$$j(t)\simeq\sigma_0 E\exp(-t/\tau_R)\,. \tag{12}$$

Consider a capacitor upon the sudden application of a field E; we know that $i=dQ/dt$ and $Q=CEd$, with the capacitance given by $C=(\epsilon_0 K/d)A$. Thus $i=(\epsilon_0 EA)dK/dt$ or $j=(E\epsilon_0)dK/dt$.

Using Eq. (12), we see that

$$j(t)=\sigma_0 E\exp(-t/\tau_R)=E\epsilon_0(dK/dt)\,, \tag{13}$$

so

$$dK=(\sigma_0/\epsilon_0)\exp(-t/\tau_R)dt\,. \tag{14}$$

To find the static dielectric constant we integrate both sides of Eq. (14) from zero to infinity:

$$K(\infty)-K(0)=(\sigma_0/\epsilon_0)\tau_R\,. \tag{15}$$

The value $K(0)$ corresponds to the value of the dielectric constant at extremely high frequency. In the limit of extremely high frequency, the dielectric constant equals one. The value $K(\infty)$ corresponds to the static dielectric constant. Substituting $\tau_R\simeq el^2/kT\mu_0$ we obtain

$$K(\infty)\simeq 1+(\sigma_0 el^2)/(\epsilon_0 kT\mu_0)\,. \tag{16}$$

The expression for the mobility μ_0 consistent with the definition for τ_0 is $\mu_0=e\tau_0/m^*$. Substituting the expression for both τ_0 and μ_0 into Eq. (16), we obtain the final result for $K(\infty)$:

$$K(\infty)\simeq 1+n_A\left(\frac{ze^2}{b\epsilon_0}\right)\frac{l^2}{kT}\,. \tag{17}$$

If we assume that the number of charge carriers per unit length (z/b) is given by

$$\frac{z}{b}=\tfrac{1}{2}e^{-(0.41\ \mathrm{eV})/kT}(3.3\times10^{-8}\ \mathrm{cm})^{-1}\,,$$

we may obtain an approximate value for l, the length of the conducting strands using the data of Figs. 10 and 11. This is the assumption made

earlier to estimate the magnitude of the non-Ohmic current. (As mentioned before, $n_A \simeq 10^{14}/\text{cm}^2$.) At room temperature, from Eq. (17) we have $K(\infty) \simeq 1 + l^2(8.0 \times 10^9\ \text{cm}^{-2})$. If $K(\infty) \simeq 5.0 \times 10^3$, $l = 8.0 \times 10^{-4}\ \text{cm} \simeq 10^5$ Å. On the basis of the electron and nuclear magnetic resonance results l was estimated to be about 3×10^5 Å. Considering the approximate nature of the dielectric-constant calculation, the agreement between theory and experiment is quite good.

The dielectric-constant model just discussed predicts that the time required for the conducting strand dipoles to form is τ_R. In measuring the dielectric constant versus frequency, one would expect the dielectric constant to drop above some critical frequency $\nu_c \simeq \tau_R^{-1} \approx (kT\mu_0/l^2 e)$.

The intrinsic mobility μ_0 is not known and the model is crude. All that can be said about the frequency dependence of the dielectric constant is that with any reasonable value for the mobility the dielectric constant will decrease above a critical frequency of order ν_c in the radio frequency range. From Fig. 11, this is clearly the case.

Attempts were made to measure the dielectric constant in the a and c directions (see Fig. 2). In both of these directions $K < 40$. Thus the dielectric constant is highly anisotropic and the direction of high dielectric constant corresponds to the direction of high electrical conductivity.

V. CONCLUSION

Quite large, well-formed single crystals of $Me\phi_3As(TCNQ)_2$ have been grown. Using these crystals it has been shown that $Me\phi_3As(TCNQ)_2$ has a large, highly anisotropic dielectric constant and a non-Ohmic conductivity. The non-Ohmic conductivity and a large dielectric constant have been observed in a number of quasi-one-dimensional conductors and semiconductors; a number of models have been proposed to explain these phenomena. None of the published models adequately explains the non-Ohmic conductivity observed in $Me\phi_3As(TCNQ)_2$. Here we have developed a model based upon charged imperfections in the conducting (TCNQ) strands which explains the data quite well. The charged imperfections act as barriers in the conducting strands. Rice and Bernasconi explain the large anisotropic dielectric constant observed in quasi-one-dimensional conductors in terms of a model based upon barriers in the conducting strands. Their model, with several modifications, explains our dielectric constant measurements very well.

The concentration of charged imperfections was assumed to be equal to the concentration of paramagnetic impurities, which were measured using magnetic resonance techniques. Reasonable agreement between the measured imperfection level and that required to explain the non-Ohmic behavior and the dielectric constant was found. A rather wide range of experimental techniques (conductivity and dielectric constant measurements, nuclear and electron spin resonance) all yield data which are consistent with and support the proposed model.

As mentioned earlier, the proposed model may also qualitatively explain much of the non-Ohmic conductivity observed by others working with similar materials. The model is consistent with the fact that non-Ohmic behavior should only occur in materials like tetrathiofulvalene tetracyanoquinodimethane (TTF-TCNQ) below the metal-to-insulator transition. As also discussed earlier, the observation that non-Ohmic behavior appears gradually as temperature is lowered in materials with small activation energies of conduction is also consistent with our model.

The model proposed may also qualitatively explain the dielectric behavior observed in some other quasi-one-dimensional materials. For example, Holczer *et al.*[21] have recently reported that the dielectric constant of quinolinium ditetracyanoquinodimethanide $[Qn(TCNQ)_2]$ can be greatly reduced by increasing the number of imperfections through neutron irradiation. They also report a temperature dependence of the dielectric constant which roughly corresponds to the temperature dependence of the conductivity. It should be pointed out that the model proposed herein does not appear to be consistent with some of the published dielectric constant work in one-dimensional conductors. Khanna *et al.*[41,42] observe a nearly temperature-independent dielectric constant in TTF-TCNQ and its disubstituted selenium derivative DSeDTF-TCNQ. A charge-density-wave model[14,15] may be more appropriate for these systems.

Thus, a very simple model, with essentially all parameters at least approximately measured or calculated, is in agreement with an extremely wide range of data obtained on high-quality crystals of $Me\phi_3As(TCNQ)_2$. In addition, the model may explain a wide range of observations in other quasi-one-dimensional conductors.

Note added

Regarding the applicability of a barrier model for non-Ohmic conductivity and giant dielectric constants in other one-dimensional systems, mention should be made of a talk given by G. Grüner shortly after the submission of this work to Physical Review.

At the March 1980 American Physical Society meeting G. Grüner discussed the giant frequency-dependent dielectric constant and the non-Ohmic

conductivity of quinolinium $(TCNQ)_2$ in terms of a barrier model which is somewhat similar to (but not the same as) the model described herein.

ACKNOWLEDGMENT

In growing the crystals used we benefited immeasurably from the advice and assistance of Dr. G. DePasquali. We are also grateful for the interest which Dr. D. B. Chesnut, Dr. L. B. Schein, Dr. Z. G. Soos, and Dr. C. P. Slichter expressed in this work and for their helpful discussions. This work is supported in part by the U.S. Department of Energy under Contract No. EY-76-C-02-1198.

*Permanent Address: Sandia National Laboratories Albuquerque, New Mexico 87185.

[1]F. Gutmann, A. M. Hermann, A. Rembaum, Nature (London) 221, 1237 (1969).
[2]J. P. Farges, A. Brau, and F. Gutmann, J. Phys. Chem. Solids 33, 1723 (1972).
[3]H. Kahlert, Solid State Commun. 17, 1161 (1975).
[4]G. D. Stucky, C. Putnick, J. Kelber, M. J. Schaffman, M. B. Salamon, G. DePasquali, A. J. Schultz, J. Williams, and T. F. Cornish, Proceedings of the Conference on Magnetism and Magnetic Materials, 1977 [Ann. N. Y. Acad. Sci. 313, 525 (1978)].
[5]J. Kurti, G. Mihaly, G. Grunner, A. Janossy (unpublished).
[6]J. E. Lane, T. R. Fico, A. Lombardo, and J. S. Blakemore, J. Chem. Phys. 69, 3981 (1978).
[7]K. Seeger and W. Maurer, Solid State Commun. 27, 603 (1978).
[8]Marshall J. Cohen and A. J. Heeger, Phys. Rev. B 16, 688 (1977).
[9]M. J. Schaffman, M. B. Salamon, G. DePasquali, A. J. Schultz, and G. D. Stucky, in *Organic Conductors and Semiconductors*, Proceedings of the International Conference, Siófak, Hungary, 1976, Vol. 65 of Lecture Notes in Physics, edited by L. Pál, G. Grüner, A. Jánossy, and J. Sólyom (Springer, New York, 1977), p. 625.
[10]Marshall J. Cohen, P. R. Newman, and A. J. Heeger, Phys. Rev. Lett. 37, 1500 (1976).
[11]M. J. Rice, S. Strassler, W. R. Schneider, in *One Dimensional Conductors*, edited by H. G. Schuster (Springer, Berlin, 1975), pp. 307–309.
[12]P. A. Lee, T. M. Rice, and P. W. Anderson, Solid State Commun. 14, 703 (1974).
[13]M. J. Rice, A. R. Bishop, J. A. Krumhansel, and S. E. Trullinger, Phys. Rev. Lett. 36, 432 (1976).
[14]M. J. Rice, in *Low Dimensional Cooperative Phenomena*, edited by H. J. Keller (Plenum, New York, 1975), p. 23ff.
[15]P. A. Lee, T. M. Rice, and P. W. Anderson, Solid State Commun. 31, 462 (1973).
[16]Robert L. Bush, Solid State Commun. 18, 1189 (1976).
[17]Robert L. Bush, Phys. Rev. B 13, 805 (1976).
[18]M. J. Rice and J. Bernasconi, Phys. Rev. Lett. 29, 113 (1972).
[19]M. J. Rice and J. Bernasconi, Phys. Lett. 38A, 277 (1972).
[20]M. J. Rice and J. Bernasconi, J. Phys. F 2, 905 (1972).
[21]K. Holczer, G. Grüner, G. Mihály, and A. Jánossy, Solid State Commun. 31, 145 (1979).
[22]E. Muller, H. Ritschel, H. Hansel, Phys. Status Solidi 33 K, 55 (1969).
[23]A. T. McPhail, G. M. Semeniuk, and D. B. Chesnut, J. Chem. Soc. A 1971, 2174.
[24]L. R. Melby, R. J. Harder, W. R. Hertler, W. Mahler, R. E. Benson, and W. E. Mochel, J. Am. Chem. Soc. 84, 3374 (1962).
[25]Patrick M. Lenahan and G. DePasquali, J. Crystal Growth 50, 739 (1980).
[26]K. Seeger, Solid State Commun. 19, 245 (1976).
[27]Murray A. Lampert and Peter Mark, *Current Injection in Solids* (Academic, New York, 1970), p. 15ff.
[28]Richard H. Bube, *Electronic Properties of Crystalline Solids* (Academic, New York, 1974), p. 466ff.
[29]L. B. Schein, Phys. Rev. B 15, 1024 (1977).
[30]A. Many and D. Rakavy, Phys. Rev. 126, 1980 (1962).
[31]E. Mertzbacher, *Quantum Mechanics*, 2nd ed. (Wiley, New York, 1970), p. 116ff.
[32]O. H. LeBlanc, J. Chem. Phys. 42, 4037 (1965).
[33]Esther M. Conwell, Phys. Rev. B 18, 1818 (1978).
[34]N. W. Ashcroft and N. D. Mermin, *Solid State Physics* (Holt, Rinehart and Winston, New York, 1976), p. 340ff.
[35]N. Bloembergen, Physica (The Hague) 15, 386 (1949).
[36]A. Abragam, *The Principles of Nuclear Magnetism* (Clarendon, Oxford, 1961), p. 378ff.
[37]D. B. Chesnut and W. D. Phillips, J. Chem. Phys. 35, 1002 (1961).
[38]J. C. Bailey and D. B. Chesnut, J. Chem. Phys. 51, 5118 (1969).
[39]A. N. Bloch, R. B. Weismann, and C. M. Varma, Phys. Rev. Lett. 28, 753 (1972).
[40]Yoicha Iida, J. Chem. Phys. 59, 1607 (1973).
[41]S. K. Khanna, A. F. Garito, and A. J. Heeger, Solid State Commun. 16, 670 (1975).
[42]S. K. Khanna, E. Ehrenfreund, A. F. Garito, and A. J. Heeger, Phys. Rev. B 10, 2205 (1974).

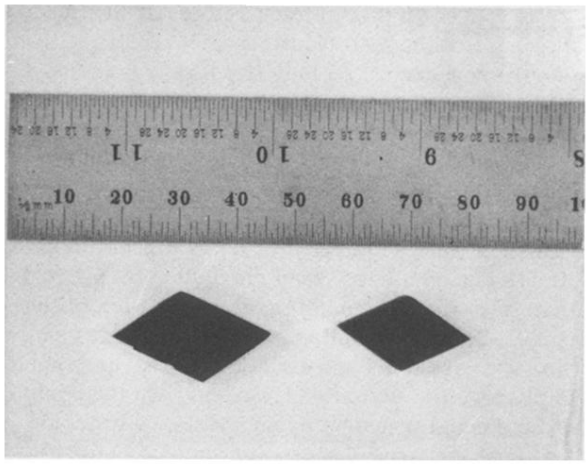

FIG. 1. Two typical crystals of $Me\phi_3As(TCNQ)_2$ as described in the text and used in this study.